

Effects of the sub-critical annealing in the microhardness and grain size of the AISI 12L14 steel

Dante Jesus Cajero-Medina¹, Jose Martín Melchor-Leal²

dante.cajero@gmail.com, jmmelchor1@gmail.com

¹Postgraduate student of the Advanced Manufacturing department, CIATEQ, Aguascalientes, México.

²Sensata Technologies Mexico Engineering Center - Member technical Staff - Design Engineer leader

ABSTRACT

The motivation of this work aims to evaluate the effect of the sub-critical annealing on grain size and microhardness in AISI 12L14 steel. In this study, 12L14 cold-drawn low carbon steel machined specimens were heat-treated at different temperatures below the temperature of transformation from perlite into austenite (Ac_1). The average grain size was measured according to the Heyn linear intercept method in ASTM E112. Microhardness was measured on the Vickers scale according to ASTM E384. Microhardness decreases and grain size increases as a function of sub-critical annealing temperature. The results show an important drop in microhardness from the sub-critical annealing temperature of 550°C. This reduction is due to recrystallization in the grains, which grow even larger with the increasing of sub-critical annealing temperature.

Keywords: AISI 12L14, sub-critical annealing, grain size, microhardness.

1. INTRODUCTION

Due to its properties, iron is the most important of the metallic elements. It is used as the main element to create all kinds of alloys, which makes it the most used and important engineering material of our time (1). The properties of iron and steel are related to their chemical composition, processing, and the resulting microstructure, this connection has been known since the beginning of the 20th century (2). For certain types of iron and steel, most of their properties depend on the microstructure, these properties are called structure-sensitive, for example, hardness, yield strength, ductility, among others (3). The relationship between the hardness and grain size is expressed by the Hall-Petch relation:

$$\sigma_y = \sigma_0 + \frac{k}{\sqrt{d}} \quad (1)$$

Where σ_y is the yield stress, σ_0 is materials constant for the starting stress for dislocation movement in a monocrystal, d is the grain size and k is a constant specific for each material (4). So far, numerous works had been done to study the effect of the resulting microstructure after different heat treatment temperatures in the mechanical properties of low carbon steels (5-8). Martínez-de-Guerenu et al (3) found that in heavily deformed (84%) cold rolled, low carbon steel, annealing temperatures equal to or lower than 500 °C, even after a long soaking time of about 13.6 hours, does not make any significative change on the hardness of the specimens, however, for the annealing carried out at 600 °C, after 10 seconds soaking, it was observed an important drop in the hardness, which is a result of the recrystallization process. This document studies the evolution in grain size and microhardness of low carbon steel AISI 12L14 as a consequence of sub-critical annealing at different temperatures below Ac_1 temperature (729.77 °C).

1.1 Problem statement

In the automotive industry is very frequent the use of AISI 12L14 cold-drawn machined cups, however, with this kind of material is very common to have cracks after processing due to the hardness of the material. It is not clearly defined where the recrystallization point is achieved in low carbon steel AISI 12L14 and is not well understood the effect in grain size and microhardness as a function of the sub-critical annealing.

2. EXPERIMENTAL PROCEDURE

2.1 Specimens

Machined specimens made of low carbon steel AISI 12L14 were used in this study, Table 1 shows the chemical composition of the steel, which complies with the ASTM A519 (9) chemical composition standard. The steel was industrially produced and cold drawn to hexagon bar form through a reduction of 10% from the original size, then machined to final shape as shown in Figure 3.

Table 1. Chemical composition of AISI 12L14 steel.

C (%)	Mn (%)	P (%)	S (%)	Si (%) *	Pb (%)	Sn (%) *
0.15	1.07	0.073	0.31	0.008	0.285	0.001

* Impurities added in the steel production process.

2.2 Groups and experiment flow

After machining, specimens were divided into 5 groups as shown in Table 2. Groups B to E were heat-treated according to each experimental temperature (T_{ex}) and Group A was not heat-treated. Then, it was measured the average grain size and microhardness of each group. Figure 1 shows the processing and test flow used for this experiment.

Table 2. Summary of sub-critical annealing experiment.

Group	Sub-critical annealing temperature (T_{ex})
A	Without heat treatment
B	260 °C
C	550 °C
D	600 °C
E	650 °C

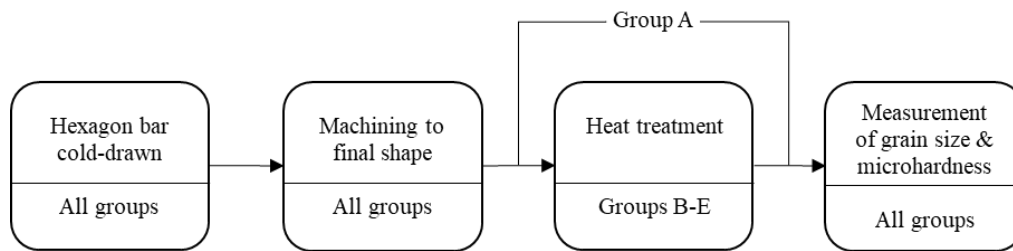


Figure 1. Thermo-mechanical processing scheme.

2.3 Sub-critical annealing

The temperatures were selected such that the effect of the heat treatment temperature on the microstructure can be observed and in order to avoid A_{c1} point, which is approximately at 729.77°C for this steel, according to calculations done in Eq. (2) using values from Table 1 with the formula suggested by Trzaska (10). Heat treatment was done according to AMS 2759/1D (11), this standard specifies parameters, conditions, and stabilization time. It was used an atmospheric oven and it was applied the following profile: 2 hours of ramp-up, 2 hours of soak in T_{ex} and for cooling down 4 hours of ramp-down at room temperature. Figure 2 illustrates the temperature profile used in the oven to apply the sub-critical annealing to the specimens.

$$A_{c1} = 742 - 29 \cdot C - 14 \cdot Mn + 13 \cdot Si + 16 \cdot Cr - 17 \cdot Ni - 16 \cdot Mo + 45 \cdot V + 36 \cdot Cu \quad (2)$$

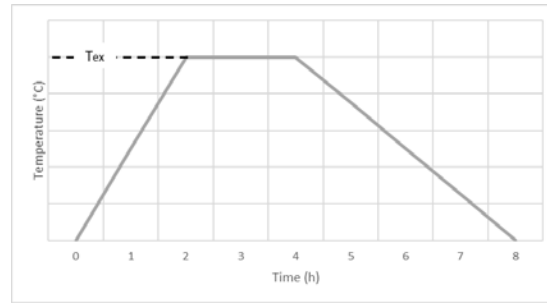


Figure 2. Heat treatment profile.

2.4 Microhardness measurements

The microhardness was measured according to the Vickers scale (HV), using a digital micro hardness tester. The location of the measurement is shown in figure 3, it was used a diamond indenter with a load of 500 grams for 15 seconds according to standard ASTM E384 (12). The measurement was repeated 10 times per sample.

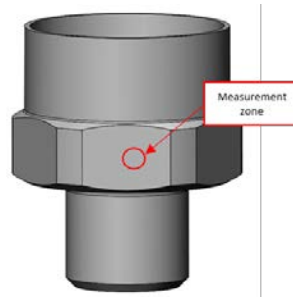


Figure 3. Machined specimen used in the study.

2.5 Average grain size measurement

The specimens were cross-sectioned, polished, and etched in nital solution at 2% for observation in optical microscopy. The average grain size measurement was done according to Heyn lineal intercept procedure in ASTM E112 (13), by analyzing micrographs taken at 400x magnification with the optical microscopy, to analyze the micrographs it was an image analysis software. For the accuracy of the measurement results, several lines were traced across different grains in each micrograph. The measurement zone is according to Figure 4c.

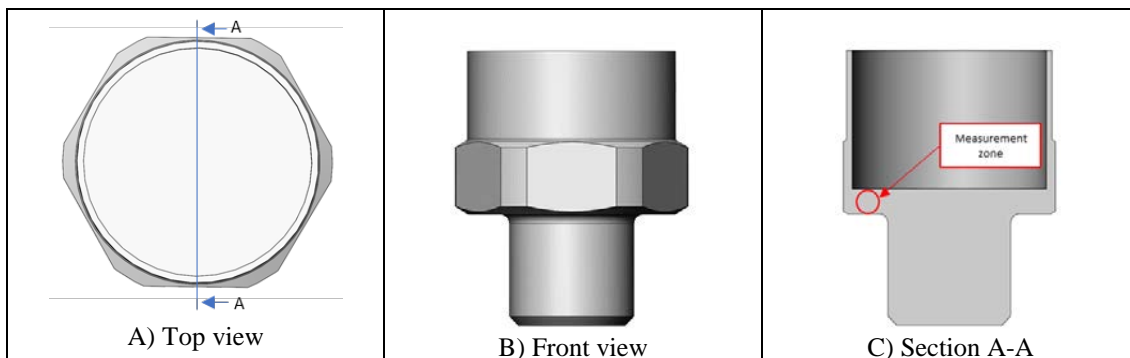


Figure 4. A) top view of specimen used in the study, B) front view of specimen C) Zone of measurement of average grain size.

3. RESULTS AND DISCUSSION

3.1 Microhardness results

Figure 5 shows the evolution of the hardness at sub-critical annealing carried out during this study. It can be seen that for the heat treatment temperature of 260°C the hardness has no big change, it has only decreased from 218 to 205.1 Vickers, in comparison to the specimens that were not heat-treated. However, for the heat treatment carried out at 550°C and 600°C, the hardness experiences an important drop of about 20%. This indicates that the recrystallization phase has been reached (3). With the sub-critical annealing temperature of 650°C, the drop in hardness is very significant, 42% compared to the specimens that were not heat-treated. The summary results are indicated in Table 3.

Table 3. Summary results of microhardness measurements.

Group	Sub-critical annealing temperature	Microhardness (HV)
A	Without heat treatment	218
B	260 °C	205.1
C	550 °C	173.5
D	600 °C	173
E	650 °C	126.5



Figure 5. Evolution of the microhardness as a function of the sub-critical annealing temperature.

3.2 Grain size results

The average grain size seen at group A of specimens without heat treatment in Table 4 is 10.52 μm, average grain size for specimens heat-treated at 260°C and 550°C remains constant, but at 600°C and 650°C grain size dramatically increased to 22.89 μm and 27.58 μm respectively, as shown in Figure 6. As can be seen in Figure 7d, the grain size of recrystallized ferrite (white) grains is larger than that in Figure 7c, indicating that the recrystallized grains grow further with the sub-critical annealing temperature (8).

Table 4 Summary of grain size measurements

Group	Heat treatment temperature	Average grain size (μm)	ASTM E112 Classification No. (G)
A	Without heat treatment	10.52	10
B	260°C	12.57	9.5
C	550°C	13.92	9.5
D	600°C	22.89	8
E	650°C	27.58	7.5

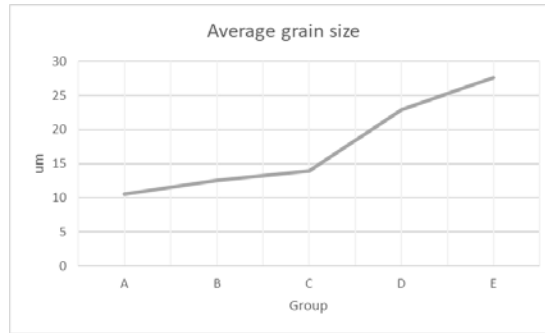


Figure 6. Evolution of the grain size as a function of the sub-critical annealing temperature.

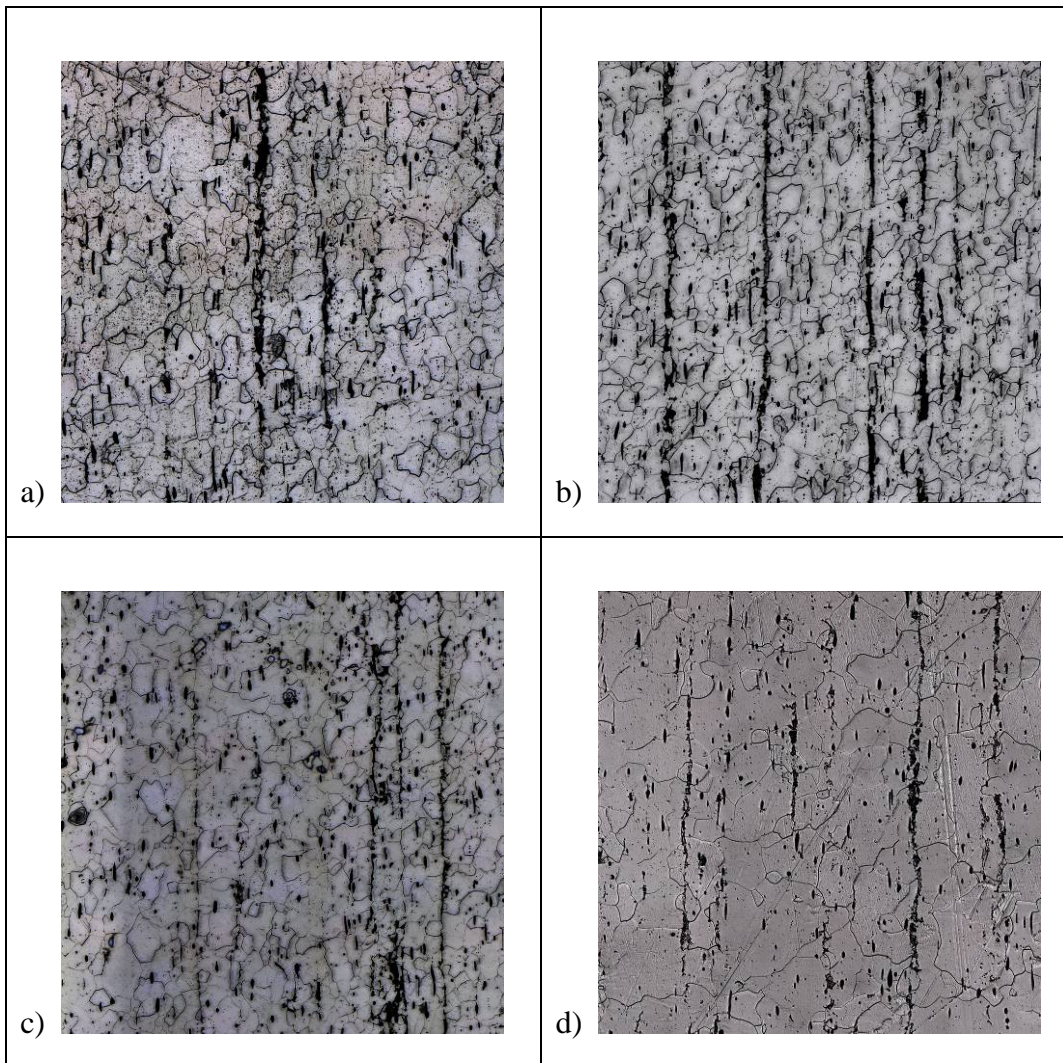


Figure 7. Micrographs showing the microstructure of the samples after different sub-critical annealing temperatures: a) 260 °C, b) 550 °C, c) 600 °C and d) 650 °C.

4. CONCLUSIONS

It can be concluded that as soon as the recrystallization is activated at the sub-critical annealing temperature of 550°C, the microhardness curve reflects the consequent softening of the steel AISI 12L14. The recrystallized ferrite grains grow 262% with the sub-critical annealing temperature of 650°C. By considering the microhardness and grain size of the steel after sub-critical annealing; it is concluded that the steel with higher grain size is characterized by lower microhardness, which is consistent with the Hall-Petch relationship.

References

- [1] Prabhudev, K. H. Handbook of heat treatment of steels. s.l. : Tata McGraw Hill Education, 1988.
- [2] Structure/Property Relationships in Irons and Steels. [book auth.] J.R. Davis. Metals Handbook Desk Edition. s.l. : ASM International, 1998, pp. 153-173.
- [3] Recovery during annealing in a cold-rolled low carbon steel. Part I: Kinetics and microstructural characterization. Martínez-de-Guerenu, A. et al. 12, 2004, Acta Materialia, Vol. 52, pp. 3657-3664.
- [4] Effect of microstructure of low-carbon steels on frictional and wear behavior. Naka, A. et al. s.l. : Tribology International, 2016, Vol. 93.
- [5] Effect of Annealing on the Microstructure and Mechanical Properties of a Low-Carbon Steel with Ultrafine Grains. Tian, J. et al. : s.n., 2017.
- [6] Effect of annealing temperature on slurry erosion resistance of ferritic X10CrAlSi18 steel. Buszko, M.H. et al. s.l. : Tribology International, 2021, Tribology International, Vol. 153.
- [7] Effect of annealing on microstructure, grain growth, and hardness of nanocrystalline Fe–Ni alloys prepared by mechanical alloying. Kotan, H. et al. 2012, Materials Science and Engineering: A, Vol. 552. ISSN 0921-5093.
- [8] Recrystallization, grain growth and austenite formation in cold rolled steels during intercritical annealing. Poyraz, O. et al. 5, s.l. : Journal of Materials Research and Technology, 2020, Vol. 9.
- [9] ASTM International. A519-17: Standard Specification for Seamless Carbon and Alloy Steel Mechanical Tubing. 2018.
- [10] Calculation of critical temperatures by empirical formulae. Trzaska, J. s.l. : Arch. Metall. Mater, 2016, Vol. 61.
- [11] SAE International. AMS 2759/1D: Heat Treatment of Carbon and Low-Alloy Steel Parts Minimum Tensile Strength Below 220 ksi (1517 MPa). 2007. pp. 1-12.
- [12] ASTM International. E 384-99: Standard Test Method for Microindentation Hardness of Materials. 2017. pp. 1-33.
- [13] ASTM International. E 112 - 96: Standard Test Methods for Determining Average Grain Size. 2017. pp. 1-26.

Author's profiles

First Author Dante Jesús Cajero-Medina received the B.Sc. degree in Mechatronics from the Monterrey Institute of Technology and Higher Education in 2016 and now he is a master's student in Advanced Manufacturing at CIATEQ, Aguascalientes, México.

Second Author Jose Martin Melchor-Leal (Ph.D.) Orcid-0000-0001-8959-1115. received the B.Sc. degree in Electronics from the Aguascalientes Institute of Technology, Mexico, in 1993 and the M.Sc. in Advanced Manufacturing from the Advanced Technology Center CIATEQ, Mexico in 2014 and Ph.D. in Advanced Manufacturing from the Advanced Technology Center CIATEQ, Mexico in 2021.